EUDET-Memo-2008-45

Calibration of Scintillator Tiles with SiPM Readout

N. D'Ascenzo*, N. Feege*,†, B. Lutz*, N. Meyer*,‡, A. Vargas Trevino*

December 18, 2008

Abstract

We report the calibration scheme for scintillator tiles with SiPM readout. Details are given on the measurements of the relevant calibration constants, including response curves for saturation correction, for a physics prototype comprising 7608 tile/SiPM cells. Dependence of the calibration coefficients on temperature drifts is investigated, based on data taken during several test beam campaigns at DESY, CERN, and FNAL. Prospects of extrapolating coefficients for temperature differences are analyzed both with and without the usage of independent temperature measurements.

*DESY, Hamburg, Germany
†University of Hamburg, Hamburg, Germany
‡e-mail: niels.meyer@desy.de

1 Introduction

An analog scintillator-steel hadron calorimeter with fine segmentation has been proposed [1] for a particle-flow optimized detector at the future ILC. First experiences with this technology exist from a small-scale technology prototype [2] and a physics prototype with 7608 channels in 38 layers of $90\times90\,\mathrm{cm}^2$ each [3]. Both test detectors are individual readout of each cell by novel Silicon Photomultipliers (SiPM). The physics prototype has been operated very successfully in several test beam campaigns at CERN and FNAL. This letter describes the strategy to individually calibrate each of the 7608 channels, the measurements of the necessary coefficient, and the extrapolation of these coefficients depending on the running conditions.
The next section briefly introduces the SiPM technology and the relevant device characteristics. The calibration scheme, the mesurements of the coefficients and the dependence on temperature and operation voltage are described in Sec. 3, followed by an introduction on the correction algorithms in Sec. 4.

2 SiPM Technology

Silicon Photo Multipliers (SiPM) are arrays of ∼1000 avalanche diodes operated in Geiger mode. In each diode (pixel), the avalanche is passively quenched by a resistor of typically few MΩ, which determines the pixel recovery time. A photo of a SiPM on its ceramic support plate and the schematics of one pixel is shown in Fig. 1. The active area of SiPMs is only $\sim1\,\mathrm{mm}^2$ in size, they are operated at a moderate bias voltage below 100 V and insensitive to magnetic fields. This enables the SiPM to be integrated directly into the scintillator, allows for a high cell granularity, and avoids long optical fibre routes.

Figure 1: SiPMs have a sensitive area of $1\times1\,\mathrm{mm}^2$ with 1136 pixels (left). Each pixel comprises a passively quenched avalanche diode operated in Geiger mode (right).

The signal of a SiPM is the product of the number of avalanches times the charge per avalanche. The number of avalanches per pixel during one readout cycle is limited by the avalanche decay time and the shaping time of the readout electronics. In the physics

prototype, the maximum number of avalanches is equal to the number of pixels, which motivates the nomenclature of '(firing) pixels' rather than 'avalanche'.
Both the charge per pixel and the probability of a single incoming photon to fire a pixel depend on the over-voltage, i.e. the excess of the bias voltage over the breakdown voltage. This voltage difference depends on the temperature (which changes the breakdown-voltage) and the applied bias voltage.
At high amplitudes, the limited number of pixels results in a non-linear relation between the number of photons hitting the SiPM surface and the measured signal. The resulting response curve is best characterized using units of pixels on both the linear (horizontal) and saturated (vertical) axis. This way, all dependence on temperature, inter-pixel cross talk[1], and quantum efficiency[2] drop out.
At the physics prototype, the SiPM is optically coupled to the tile by a wafelength shifting fibre, which is inserted into a groove on the tile surface. For the generation of SiPMs used, this was necessary due to the low quantum efficiency for blue light as emitted by the scintillator. Recently, blue-sensitive SiPMs are available, which in principle allow direct coupling. However, the fibre also enhances the geometrical uniformity of the cell response. One $3 \times 3\text{cm}^2$ tile with fibre and SiPM is shown in Fig. 2.

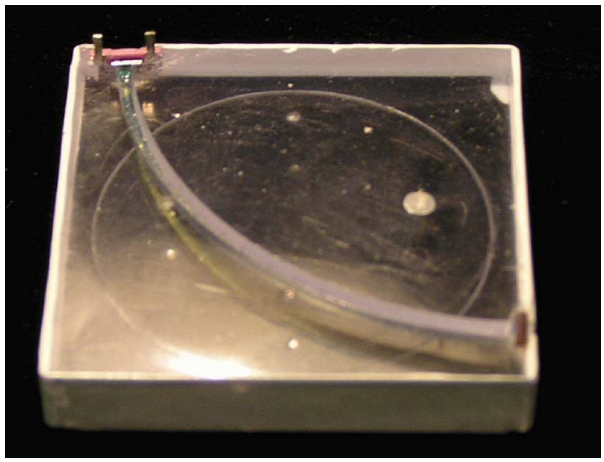

Figure 2: A wavelength-shifting fiber inserted into a groove in the scintillator tile surface collects the UV scintillating light, converts it to green and iluminates a SiPM integrated into the tile edge (upper left).

[1] inter-pixel cross talk: optical photons from a Geiger avalanche can reach neighbouring pixels and initiate a second avalanche; the occurance depends on bias voltage and temperature

[2] quantum efficiency: here, quantum efficiency denotes the probability that a single photon hitting the SiPM surface initiates an avalanche. This includes constant effects like the geometrical efficiency, but also temperature and bias-voltage dependent effects like the Geiger efficiency

3 Calibration Scheme

The calibration of a single cell depends on three individual measurements:

1. Gain calibration A_{pix}, i.e. the average signal from a single avalanche. This is the intrinsic SiPM scale and is needed to correct for saturation effects

2. Response curve $f(A)$, i.e. the measured signal as a function of the number of photons reaching the SiPM surface. The SiPM response is calibrated to pixel, and the light intensity is calibrated to yield $F(a) = a$ for low amplitudes a.

3. Mip calibration A_{mip}, i.e. the most probable signal from a minimum ionizing particle crossing the cell at normal incidence. This is a simple scale easily defined both in data and simulation, which at the same time equalizes all channels.

Measured amplitudes A_{raw} are calibrated to the Mip level by

$$A\,[\mathrm{Mip}] = f^{-1}(A_{raw}/A_{pix}) \cdot \frac{A_{pix}}{A_{mip}} \tag{1}$$

For low measured amplitudes, the response curve is close to unity and the calibrated amplitude is given by $A\,[\mathrm{Mip}] = A_{raw}/A_{mip}$. It can be seen that any uncertainty on the Mip calibration measurement contributes to the uncertainty on the calibrated amplitude by the same relative amount, while uncertainties on the gain calibration and response curve measurements only propagate to the fraction of the calibrated amplitude arising from the non-linearity correction.
The quantity A_{pix}/A_{mip} is refered to as 'light yield' and describes the most probable number of pixels firing in a given cell at passage of a minimum ionizing particle, i.e. describes the SiPM characteristics on the phyics scale. The bias voltages applied to the calorimeter modules is chosen such that the light yield of all channels is neither too small (< 10) to avoid reduced signal efficiency due to statistical fluctuations nor too large (> 20) to fit the maximum SiPM signal inside the dynamic range of the electronics. In the following, details will be given on the determination of the three ingredients to the calibration algorithm.

3.1 Gain calibration

The gain calibration is measured using the LED calibration system with low photon intensities and a larger amplification factor of the readout electronics. An example for an arbitrary channel is shown in Fig. 3. Due to the larger pre-amplification, the signal from small integer numbers of avalanches are clearly distinguished. Several Gauss functions are used to fit the spectrum in each channel, where the distance ΔA between two adjacent peaks determines the signal per avalanche. Together with the inter-calibration IC of the two amplification factors, this number gives the gain calibration factor

$$A_{pix} = \Delta A / IC. \tag{2}$$

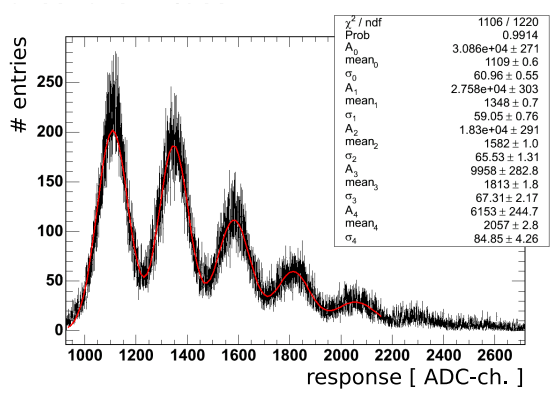

Figure 3: Example for a gain calibration measurement from one arbitrary channel, with the applied fit shown as solide line. Separated peaks from integer numbers of avalanches are clearly distinguished.

The gain calibration data for all channels is taken simutaneously, and the usage of the LED calibration system allows data taking rates at the DAQ limit. With the current protoype, a gain calibration run takes about half an hour only, which allows frequent repetition. Correction for temperature drifts are only necessary when the repetition interval is long compared to time scale of temperature changes (e.g. day-night fluctuations).
From many gain calibrations measured over a broad range of bias voltage settings and temperature conditions, the specific slope of the calibration w.r.t. these circumstances could be measured. The gain variation of an example channel with temperature is shown in Fig. 4 (left) for two bias voltages differing by 0.5 V. The right side of the same figure shows the variation with voltage for the same channel from two scans at different temperatures ($\Delta T \sim 2\,\mathrm{K}$).

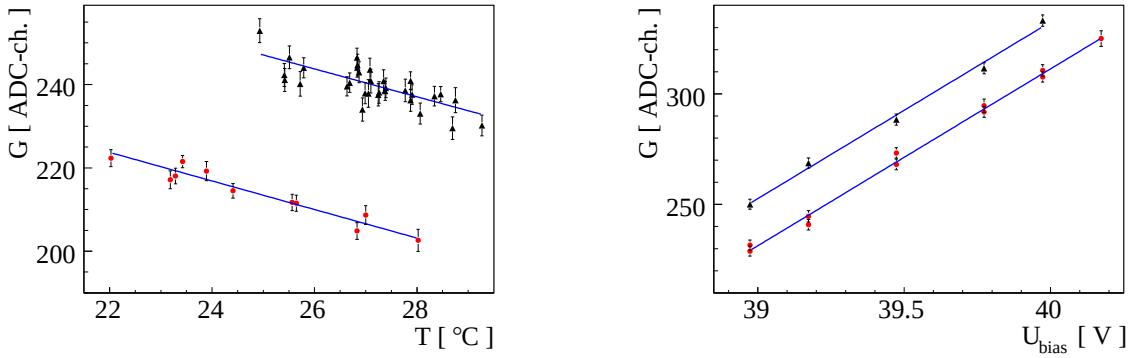

Figure 4: Dependence of the gain on temperature (left) for two different bias voltages ($\Delta U = 0.5\,\mathrm{V}$) and on bias voltage (right) at two different temperatures ($\Delta T = 2\,\mathrm{K}$). All data is shown for the same randomly picked channel.

3.2 Response curve

The response curve of each SiPM has been measured prior to mounting on tiles using a test-bench setup. Compared to later in-situ measurements using the LED calibration system of the fully comissioned prototype, a lower maximum amplitude has been observed. This was found to originate from partial ilumination of the SiPM surface by the light cone from the wavelength-shifting fibre after mounting the SiPM on its tile. Figure 5 shows the two response curves from the test-bench and in-situ measurements for one random channel, respectively. The correlation between the maximum amplitudes, indicated by the dotetd blue lines, is shown in Fig. 6 for about 5000 channels.

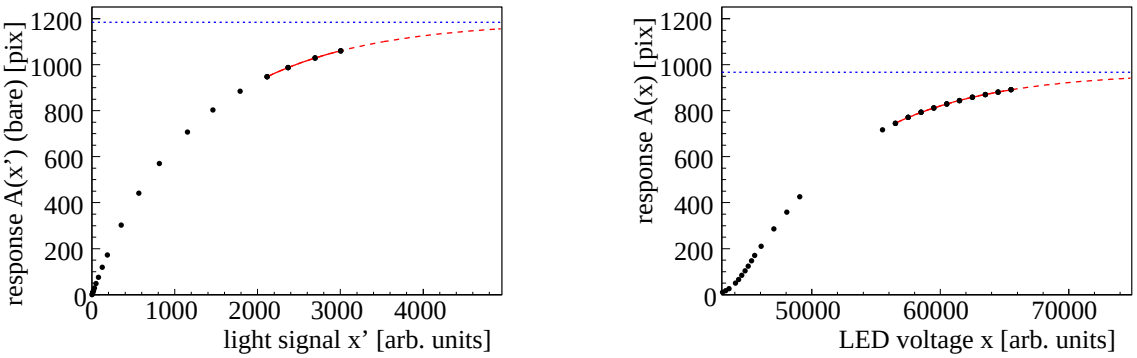

Figure 5: Single channel example for the response curve measured with the bare SiPM on a test-bench (left) and in-situ using the LED calibration system of the fully integrated HCal prototype (right). Due to incomplete ilumination of the SiPM after mounting on the tile, the number of effective pixels, i.e. the maximum amplitude in units of firing pixels, is reduced.

Neither the test-bench nor the in-situ response curves are suitible for correcting the SiPM signal. The test-bench measurement does not describe the effectively reduced number of working/iluminated pixels. The in-situ measurement correlates the SiPM amplitude to the voltage applied to the LEDs, which has a non-linear and non-trivial relation to the number of photons hitting the SiPM. The LED signal is monitored by PIN diodes. However, the dynamic range of the PIN diode readout is not sufficient to calibrate the LED signal over the full dynamic range. Therefore, both measurements are combined into a virtual response curve, which is then used to correct the SiPM saturation: The functional form is taken from the test-bench measurement, while the vertical axis gets scaled by the ratio of maximum amplitudes from in-situ and test-bench measurements, respectively.

3.3 Mip calibration

The Mip calibration constant is determined using muon beam data. The resulting spectrum for an example channel is shown in Fig. 7 using only those events where

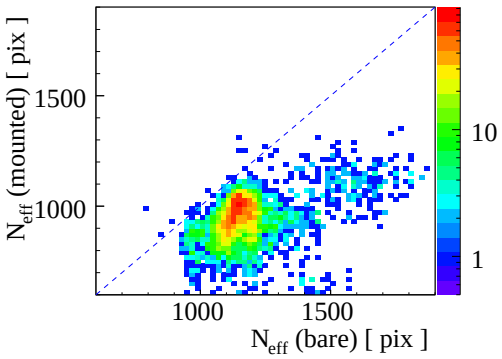

Figure 6: Comparison of the maximum amplitude from test-bench and in-situ measurements of the response curve for about 2/3 of all channels comissioned in the HCal test beam prototype. No correlation is evident, as is expected from the individual integration process of SiPM and tile.

the muon crossed the respective tile. The spectrum is fitted with a landau function convoluted with a Gaussian, and the Mip calibration constant is extracted as the most probable value of the fitted function.
Every muon event contributes to the calibration of only 38 out of 7608 channels (one per layer) and depends on the beam luminosity. Therefore, the measurement of a complete set of Mip coefficients takes several hours to days even when the beam spread coveres the whole detector surface. Frequent repetitions, especially at a colliding beam detector, thus are not realistic. Changes in the operation conditions, especially temperature drifts, therefore will have to be corrected using independent 'standard candles', which will be discussed in more detail in Sec. 4.

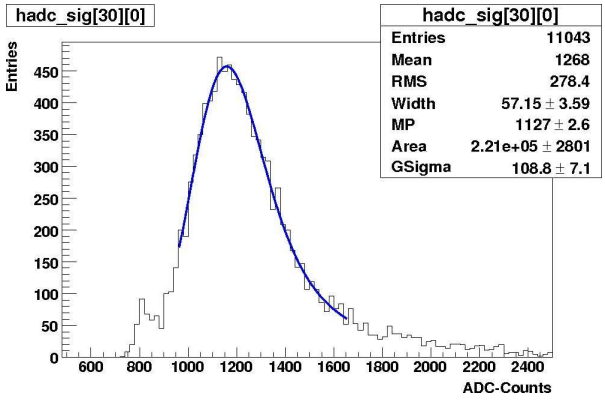

Figure 7: Example of a Mip calibration measurement from one arbitrary channel. The fit as explained in the text is shown as solid line.

Dedicated scans have been recorded to determine the channel-by-channel variations on temperature and bias voltage. Results for an example channel are shown in Fig. 8

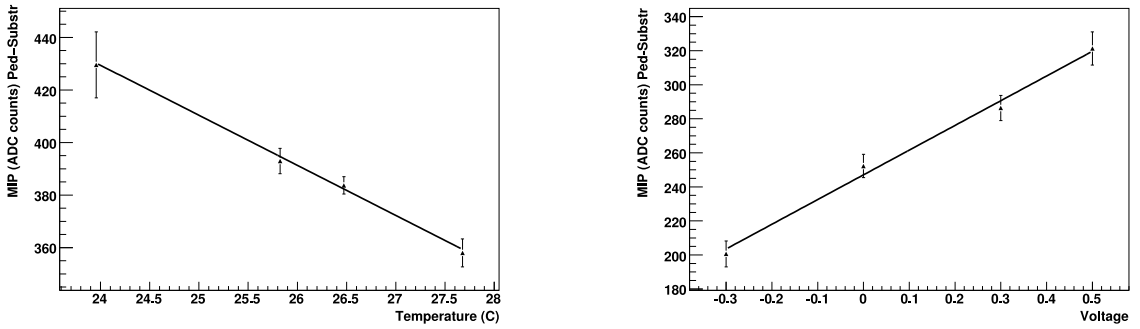

Figure 8: Dependence of the Mip coefficient on temperature (left) and voltage (right).

4 Temperature extrapolation

In general, the temperature between recording a calibration run on the one hand side and to-be-calibrated data on the other can change[3]. In order to obtain calibration constants matching to-be-calibrated data, the constants are extrapolated to the different conditions rather than applying a later correction to calibrated data. In the following, it will be shown that this is a valid approach when the temperature is known from an independent measurement.

After working-point optimization (see comment on the ligh yield in section 3) at the beginning of a test beam campaign, the bias voltage is kept fixed for the rest of the period. Therefore, temperature drift is the only source of change in SiPM characteristics between calibration and beam data. Calibration constants are extrapolated to the temperature conditions valid at the time where the data to be calibrated where recorded using the measured slopes described above.

For Fig. 9, two gain and Mip measurments at different temperatures are compared, respectively. The open histograms show the channel-by-channel difference of the two measurements. For the filled histograms, the results from one measurement have been extrapolated to the temperature conditions of the second measurement before the comparison. On average, the differences both in the Mip and in the gain coefficients vanish without introducing a sizeable additional spread.

This procedure requires knowledge of the detector temperature. This is granted thanks to the temperature sensors in the current prototype, but is desirebale to be spared for a colliding beam detector. In principle, the drift of the Mip calibration can be deduced from the drift of the gain coefficients, which can be measured rather frequent. The results of this extrapolation is shown in Fig. 10 using the same two Mip measurements as before. A small fraction of the drift remains uncorrected. In addition, a non-negligible extra contribution to the uncertainty of the (extrapolated) calibration constant is observed.

[3]For the physical prototype, the operation voltage is not altered during contenous running. Floating operation voltage would have to be monitored and corrected for analogous to the correction for temperature drift described here.

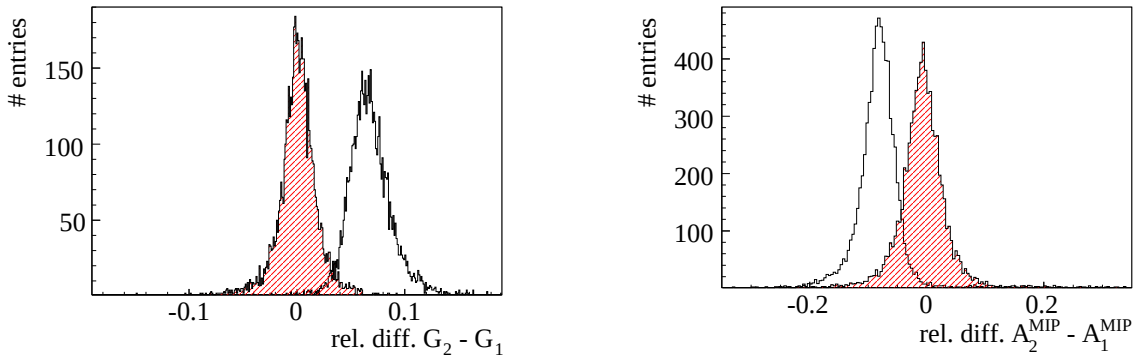

Figure 9: Comparison of two gain (left) and Mip (right) measurements at different temperatures. The open histograms show the difference of the raw measurements. For the filled histograms, the values of one measurement have been extrapolated by the temperature difference before comparison.

More studies will be needed for final judgement about the usability of this correction strategy.

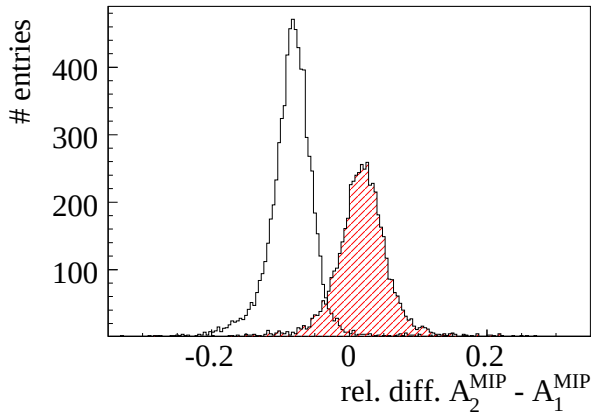

Figure 10: Comparison of two Mip measurements at different temperatures. For both sets, gain measurements at similar conditions are available. The open histogram shows the difference of the raw measurements. For the filled histograms show the difference after one Mip measurement has been extrapolated using the difference in the accompagnying gain measurements.

5 Conclusion

A physics prototype of an analog hadron calorimeter optimized for particle flow and based on scintillator tiles with SiPM readout has been constructed and successfully

operated at several test beam campaigns. The calibration procedure and the relevant measurements of channel-by-channel calibration coefficients have been introduced. The dependence of gain and Mip coefficients with temperature and bias voltage have been determined.
It has been shown that the drift of calibration coefficients with temperature can be corrected for without introducing additional uncertainties on the calibration, as long as an independent measurement of the temperature is available. Results from an indirect extrapolation using frequent gain measurements shows potential, but needs to be investigated further before the requirement for temperature measurements can be dropped for a large-scale colliding beam detector.
This letter described the calibration procedure for a single cell, although results for the calibration coefficients have been measured in the completely assembled physics prototype. The validity of this procedure and understanding of the detector as a whole can only be established by comparison of electromagnetic test shower data with simulations. The status of this ongoing analysis will be presented in a separate EUDET-Memo.

Acknowledgement

This work is supported by the Commission of the European Communities under the 6^{th} Framework Programme "Structuring the European Research Area", contract number RII3-026126.

References

[1] K. Gadow et al., "JRA3 Hadronic Calorimeter Technical Design Report", EUDET-Memo-2008-02.

[2] V. Andreev et al., Nucl. Instrum. Meth. A **540** (2005), 368.

[3] C. de La Taille et al., "JRA3 Calorimeter Conceptual Report", EUDET-Memo-2007-08.